

Supersymmetric Lepton Flavour Violation in Low-Scale Seesaw Models

Amon Ilakovac^a and Apostolos Pilaftsis^b^aUniversity of Zagreb, Department of Physics, Bijenička cesta 32, P.O. Box 331, Zagreb, Croatia^bSchool of Physics and Astronomy, University of Manchester, Manchester M13 9PL, United Kingdom

We study a new supersymmetric mechanism for lepton flavour violation in μ and τ decays and $\mu \rightarrow e$ conversion in nuclei, within a minimal extension of the MSSM with low-mass heavy singlet neutrinos and sneutrinos. We find that the decays $\mu \rightarrow e\gamma$, $\tau \rightarrow e\gamma$ and $\tau \rightarrow \mu\gamma$ are forbidden in the supersymmetric limit of the theory, whereas other processes, such as $\mu \rightarrow eee$, $\mu \rightarrow e$ conversion, $\tau \rightarrow eee$ and $\tau \rightarrow e\mu\mu$, are allowed and can be dramatically enhanced several orders of magnitude above the observable level by potentially large neutrino Yukawa coupling effects. The profound implications of supersymmetric lepton flavour violation for present and future experiments are discussed.

PACS numbers: 11.30Hv, 12.60Jv, 13.15.+g

One of the best theoretically motivated scenarios of new physics is the Minimal Supersymmetric Standard Model (MSSM), softly broken at the TeV scale. Its main virtues are that it provides a quantum-mechanically stable solution to the so-called gauge hierarchy problem, predicts gauge-coupling unification more accurately than the Standard Model (SM) does and offers a hopeful perspective for a consistent quantization of gravity by means of supergravity (SUGRA) and superstrings [1].

Nevertheless, the low-energy sector of the MSSM needs be extended in order to accommodate the low-energy neutrino oscillation data. One popular extension is the one that realizes the famous seesaw mechanism [2], where the smallness of the observable neutrinos is counterbalanced by the presence of ultraheavy right-handed neutrinos $N_{1,2,3}$ with Majorana masses that are two to four orders of magnitude below the grand unification theory (GUT) scale $M_{\text{GUT}} \sim 10^{16}$ GeV. The leptonic superpotential part for this extension is

$$W_{\text{lepton}} = \hat{E}^C \mathbf{h}_e \hat{H}_d \hat{L} + \hat{N}^C \mathbf{h}_\nu \hat{L} \hat{H}_u + \hat{N}^C \mathbf{m}_M \hat{N}^C, \quad (1)$$

where $\hat{H}_{u,d}$, \hat{L} , \hat{E} and \hat{N}^C denote the two Higgs-doublet superfields, the three left- and right-handed charged-lepton superfields and the three right-handed neutrino superfields, respectively. Note that the Yukawa couplings $\mathbf{h}_{e,\nu}$ and the Majorana mass parameters \mathbf{m}_M are 3×3 complex matrices. In a minimal SUGRA seesaw model, lepton flavour violation (LFV), such as $\mu \rightarrow e\gamma$ and $\mu \rightarrow eee$, originates from off-diagonal renormalization-group effects induced by the neutrino Yukawa couplings \mathbf{h}_ν on the soft supersymmetry (SUSY) breaking mass matrices $\tilde{\mathbf{M}}_{L,E}^2$ and the trilinear couplings $\mathbf{h}_e \mathbf{A}_e$ [3, 4]. However, if the soft SUSY-breaking parameters $\tilde{\mathbf{M}}_{L,E}^2$ and \mathbf{A}_e were flavour diagonal or proportional to the 3-by-3 identity matrix $\mathbf{1}$ at $\mathbf{m}_M \approx m_N \mathbf{1}$, with $m_N \gtrsim 10^{12}$ GeV, all low-energy charged LFV phenomena would be extremely suppressed by factors

m_ν/m_N [5], where $m_\nu \lesssim 0.1$ eV is the light-neutrino mass scale.

In this Letter we study a new supersymmetric mechanism for lepton flavour violation (SLFV) which becomes dramatically enhanced in low-scale seesaw extensions of the MSSM. As we will show, the new important feature of SLFV is that it does not vanish in the supersymmetric limit of the theory, giving rise to distinctive predictions for charged LFV in present and future experiments, such as MEG [6] and PRISM [7].

In low-scale seesaw models of interest here [8, 9, 10, 11], the smallness of the light neutrino masses is accounted for by natural, quantum-mechanically stable cancellations due to the presence of approximate lepton flavour symmetries [11, 12], whereas the Majorana mass scale m_N can be as low as 100 GeV. Most interestingly, in these models LFV transitions from a charged lepton $l = e, \mu, \tau$ to another $l' \neq l$ are generically enhanced by the ratios [13, 14, 15]

$$\Omega_{ll'} = \frac{v_u^2}{2m_N^2} (\mathbf{h}_\nu^\dagger \mathbf{h}_\nu)_{ll'}, \quad (2)$$

where $v_u/\sqrt{2} \equiv \langle H_u \rangle$ is the vacuum expectation value (VEV) of the Higgs doublet H_u , with $\tan \beta \equiv \langle H_u \rangle / \langle H_d \rangle$. Here we will set limits on the off-diagonal entries of $\Omega_{e\mu}$, $\Omega_{\mu\tau}$ and $\Omega_{e\tau}$ that are derived from the non-observation of LFV in μ and τ decays and of $\mu \rightarrow e$ conversion in nuclei [16].

To be able to understand the profound implications of SLFV, we assume that the singlet neutrino sector of the low-scale seesaw model is exactly supersymmetric. This assumption is a good approximation, as long as $m_N \gg M_{\text{SUSY}}$, where $M_{\text{SUSY}} = 0.1\text{--}1$ TeV denotes a typical soft SUSY-breaking mass for the $U(1)_Y$ and $SU(2)_L$ gauginos, \tilde{B} and $\tilde{W}_{1,2,3}$, and for the left-handed sneutrinos, $\tilde{\nu}_{e,\mu,\tau}$. As an illustrative scenario, we consider that m_N is much larger than the superpotential $\hat{H}_u \hat{H}_d$ -mixing

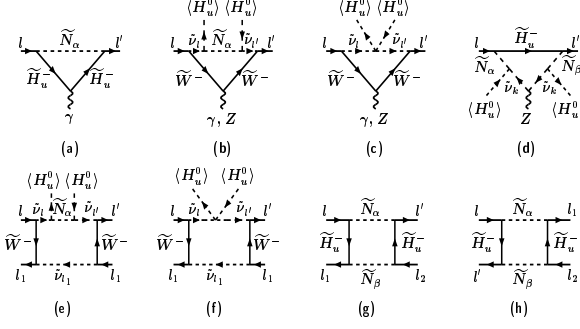


FIG. 1: Feynman graphs giving rise to leading SLFV effects in the lowest order of an expansion in $\langle H_u^0 \rangle$. Not shown are diagrams obtained by replacing the tilted SUSY states \tilde{H}_u^- , \tilde{W}^- , \tilde{N}_α and $\tilde{\nu}_l$ with their untilted counterparts.

parameter μ and that $\tilde{M}_{L,E}^2$ and \mathbf{A}_e are flavour conserving, e.g. proportional to $\mathbf{1}$ at the energy-scale m_N .

Within the above simplified but realistic framework, we may calculate the leading effects of SLFV in the lowest order of a series expansion of the Higgs VEV v_u . We ignore charged Higgs effects which are subdominant in a heavy-neutrino mass expansion. Detailed analytic results including this and other subleading contributions will be given in a separate communication [18]. The Feynman graphs that contribute to $\gamma l' l$ - and $Z l' l$ -couplings and box diagrams to leading order in the $SU(2)_L$ gauge coupling g_w and the neutrino Yukawa coupling \mathbf{h}_ν are shown in Fig. 1. The pertinent transition amplitudes may be cast into the form:

$$\begin{aligned} \mathcal{T}_\mu^{\gamma l' l} &= \frac{e \alpha_w}{8\pi M_W^2} \bar{l}' \left(F_\gamma^{l' l} q^2 \gamma_\mu P_L + G_\gamma^{l' l} i \sigma_{\mu\nu} q^\nu m_l P_R \right) l, \\ \mathcal{T}_\mu^{Z l' l} &= \frac{g_w \alpha_w}{8\pi \cos \theta_w} F_Z^{l' l} \bar{l}' \gamma_\mu P_L l, \\ \mathcal{T}_l^{l' l_1 l_2} &= -\frac{\alpha_w^2}{4M_W^2} F_{\text{box}}^{l' l_1 l_2} \bar{l}' \gamma_\mu P_L l \bar{l}_1 \gamma^\mu P_L l_2, \end{aligned} \quad (3)$$

where $P_{L(R)} = \frac{1}{2} [1 - (+) \gamma_5]$, $\alpha_w = g_w^2/(4\pi)$, e is the electromagnetic coupling constant, $M_W = g_w \sqrt{v_u^2 + v_d^2}/2$ is the W -boson mass, θ_w is the weak mixing angle and $q = p_{l'} - p_l$ is the photon momentum. In addition, the formfactors $F_\gamma^{l' l}$, $G_\gamma^{l' l}$, $F_Z^{l' l}$ and $F_{\text{box}}^{l' l_1 l_2}$ receive contributions from both the heavy neutrinos $N_{1,2,3}$ and the right-handed sneutrinos $\tilde{\nu}_{1,2,3}$. In the Feynman gauge [19], these are individually given by

$$\begin{aligned} (F_\gamma^{l' l})^N &= \frac{\Omega_{l'l}}{6 s_\beta^2} \ln \frac{m_N^2}{M_W^2}, \\ (F_\gamma^{l' l})^{\tilde{N}} &= \frac{\Omega_{l'l}}{3 s_\beta^2} \ln \frac{m_N^2}{\tilde{m}_h^2}, \\ (G_\gamma^{l' l})^N &= -\Omega_{l'l} \left(\frac{1}{3 s_\beta^2} + \frac{1}{6} \right), \end{aligned} \quad (4)$$

$$(G_\gamma^{l' l})^{\tilde{N}} = \Omega_{l'l} \left(\frac{1}{3 s_\beta^2} + \frac{M_W^2}{6 \tilde{m}_1^2} \right), \quad (5)$$

$$(F_Z^{l' l})^N = -\frac{3 \Omega_{l'l}}{2} \ln \frac{m_N^2}{M_W^2} - \frac{(\Omega^2)_{l'l}}{2 s_\beta^2} \frac{m_N^2}{M_W^2},$$

$$(F_Z^{l' l})^{\tilde{N}} = \frac{\Omega_{l'l}}{2} \ln \frac{m_N^2}{\tilde{m}_1^2} + \frac{(\Omega^2)_{l'l}}{4 s_\beta^2} \frac{m_N^2}{M_W^2} \ln \frac{m_N^2}{\tilde{m}_2^2}, \quad (6)$$

$$\begin{aligned} (F_{\text{box}}^{l' l_1 l_2})^N &= -\Omega_{l'l} \delta_{l_1 l_2} - \Omega_{l_1 l} \delta_{l' l_2} \\ &\quad + \frac{1}{4 s_\beta^4} \left(\Omega_{l'l} \Omega_{l_1 l_2} + \Omega_{l_1 l} \Omega_{l' l_2} \right) \frac{m_N^2}{M_W^2}, \end{aligned}$$

$$\begin{aligned} (F_{\text{box}}^{l' l_1 l_2})^{\tilde{N}} &= -\frac{M_W^2}{\tilde{m}^2} \left(\Omega_{l'l} \delta_{l_1 l_2} + \Omega_{l_1 l} \delta_{l' l_2} \right) \\ &\quad + \frac{1}{4 s_\beta^4} \left(\Omega_{l'l} \Omega_{l_1 l_2} + \Omega_{l_1 l} \Omega_{l' l_2} \right) \frac{m_N^2}{M_W^2}. \end{aligned} \quad (7)$$

In the above, it is $s_\beta \equiv \sin \beta$, $\tilde{m}_W^2 = \max(M_W^2, g_w^2 v_u^2/2)$, $\tilde{m}_h^2 = \max(\mu^2, g_w^2 v_u^2/2)$, $\tilde{m}_{1,2}^2 = \max(\tilde{m}_{W,h}^2, M_{\tilde{\nu}}^2)$ and $\tilde{m}^2 = \max(2M_{\tilde{\nu}}^2, \tilde{m}_W^2)$, where $M_{\tilde{\nu}}$ is a common soft SUSY mass for $\tilde{\nu}_{e,\mu,\tau}$. In the SUSY limit which requires a vanishing μ -parameter and $\tan \beta = 1$ [20, 21], all the mass parameters $\tilde{m}_{W,h}^2$, $\tilde{m}_{1,2}^2$ and \tilde{m}^2 become equal to $M_W^2 = g_w^2 v_u^2/2$.

It is now important to notice that the photonic dipole formfactor $G_\gamma^{l' l}$ vanishes in the SUSY limit when the heavy neutrino and sneutrino contributions given in (5), $(G_\gamma^{l' l})^N$ and $(G_\gamma^{l' l})^{\tilde{N}}$, are added together. This result is a direct consequence of a non-renormalization theorem of SUSY [22]. Thus, if SUSY is the dominant source for LFV in nature, photonic charged lepton decays, such as $\mu \rightarrow e \gamma$, $\tau \rightarrow e \gamma$ and $\tau \rightarrow \mu \gamma$, become practically forbidden transitions. In reality, SUSY is softly broken and these decay rates will strongly depend on the details of the soft SUSY-breaking sector. It is remarkable here, however, that even a flavour conserving soft SUSY-breaking sector for the low-scale seesaw models under study can cause sizeable LFV.

Another important observation pertains the actual strength of the neutrino Yukawa couplings \mathbf{h}_ν . If $|\mathbf{h}_\nu| \gtrsim g_w \approx 0.65$, then terms of order $(\Omega_{l'l})^2 \propto (\mathbf{h}_\nu^\dagger \mathbf{h}_\nu)_{l'l}^2$ will dominate the Z -boson and box-mediated transition amplitudes given in (3) [14]. Therefore, the central goal of this study is to identify the key phenomenological features that would enable one to distinguish whether SLFV originates from small or potentially large neutrino Yukawa couplings.

To obtain predictions for the LFV observables $B(\mu^- \rightarrow e^- \gamma)$, $B(\tau^- \rightarrow e^- \gamma)$, $B(\mu^- \rightarrow e^- e^- e^+)$, $B(\tau^- \rightarrow e^- e^- e^+)$ and $B(\tau^- \rightarrow e^- \mu^- \mu^+)$, we use the analytic expressions (4.9) and (4.10) of [14], along with the formfactors given in (4)–(7). The predicted rate $R_{\mu e}$ for coherent $\mu \rightarrow e$ conversion in a nucleus with atomic numbers (N, Z) may be calculated by

$$R_{\mu e} = \frac{\alpha^3 \alpha_w^4 m_\mu^5 |F(-m_\mu^2)|^2}{16 \pi^2 M_W^4 \Gamma_{\text{capt}}} \frac{Z_{\text{eff}}^4}{Z} |Q_W|^2, \quad (8)$$

where $\alpha = e^2/(4\pi)$, Z_{eff} is the effective atomic number of coherence [23], $F(-m_\mu^2)$ is a nucleus-dependent nuclear form factor [24] and Γ_{capt} is the total muon capture rate. In addition, $Q_W = V_u(2Z + N) + V_d(Z + 2N)$ is the weak matrix element, where

$$V_u = \frac{2}{3}s_w^2(F_\gamma^{\mu e} - G_\gamma^{\mu e} - F_Z^{\mu e}) + \frac{1}{4}(F_Z^{\mu e} - F_{\text{box}}^{\mu euu}),$$

$$V_d = -\frac{1}{3}s_w^2(F_\gamma^{\mu e} - G_\gamma^{\mu e} - F_Z^{\mu e}) - \frac{1}{4}(F_Z^{\mu e} + F_{\text{box}}^{\mu edd}), \quad (9)$$

with $s_w \equiv \sin \theta_w$. The leading contributions to the form-factors $F_{\text{box}}^{\mu euu}$ and $F_{\text{box}}^{\mu edd}$ pertinent to the up- and down-quarks, respectively, are obtained by calculating the W - and \tilde{W} -mediated box graphs analogous to Fig. 1. More explicitly, we find

$$(F_{\text{box}}^{\mu euu})^N = -4(F_{\text{box}}^{\mu edd})^N = 4\Omega_{e\mu},$$

$$(F_{\text{box}}^{\mu euu})^{\tilde{N}} = \frac{2M_W^2 \tilde{m}_W^2}{\tilde{M}_Q^4} \Omega_{e\mu}, \quad (10)$$

$$(F_{\text{box}}^{\mu edd})^{\tilde{N}} = -\frac{M_W^2}{2\tilde{M}_Q^2} \Omega_{e\mu},$$

where we assumed that $|\tilde{m}_W| \ll \tilde{M}_Q \approx M_{\tilde{\nu}}$, with \tilde{M}_Q being a common soft SUSY-breaking mass for the left-handed up and down squarks in the loop.

In our numerical estimates, we fix $\tilde{M}_Q = M_{\tilde{\nu}} = 200$ GeV, $\mu = M_{\tilde{W}} = 100$ GeV and $\tan \beta = 3$. We first analyze the impact of SLFV on $\mu \rightarrow e$ transitions. We consider a conservative scenario with $\Omega_{ee} = \Omega_{\mu\mu} = \Omega_{e\mu}$ and $\Omega_{\tau\tau} = 0$, which yields the weakest limits on $\Omega_{e\mu}$. To this end, we present in Fig. 3 exclusion contours for $\Omega_{e\mu}$ versus m_N derived from present experimental limits and future sensitivities: $B(\mu^- \rightarrow e^- \gamma) < 1.2 \times 10^{-11}$ [25] (upper horizontal line), $B(\mu^- \rightarrow e^- \gamma) \sim 10^{-13}$ [6] (lower horizontal line), $B(\mu^- \rightarrow e^- e^- e^+) < 10^{-12}$ [25] (dashed line). We also include constraints from the non-observation of $\mu \rightarrow e$ conversion in $^{48}_{22}\text{Ti}$ and $^{197}_{79}\text{Au}$ [26], $R_{\mu e}^{\text{Ti}} < 4.3 \times 10^{-12}$ [27] (dash-dotted) and $R_{\mu e}^{\text{Au}} < 7 \times 10^{-13}$ [28] (dash-double-dotted), as well as potential limits from a future sensitivity to $R_{\mu e}^{\text{Ti}}$ at the 10^{-18} level [7] (lower dash-dotted line). The areas lying above the contours are excluded by the above considerations. In the upper panel of Fig. 2, the loop effects from both $N_{1,2,3}$ and $\tilde{N}_{1,2,3}$ are considered, whereas in the lower one only these from $N_{1,2,3}$ are taken into account. Finally, the diagonal dotted line indicates the regime where terms $\propto (\Omega_{\nu l})^2$ dominate the LFV observables, whilst the area above the diagonal solid line represents a non-perturbative regime with $\text{Tr}(\mathbf{h}_\nu^\dagger \mathbf{h}_\nu) > 4\pi$, which limits the validity of our predictions.

Figure 2 also shows the importance of synergy among the different LFV experiments. In particular, we find an area of cancellation in the predicted value for the $\mu \rightarrow e$ conversion rate in nuclei for $m_N \sim 3$ TeV. This area is somehow covered by the present limits from the $\mu \rightarrow eee$ experiment. Instead, the current exclusion limit

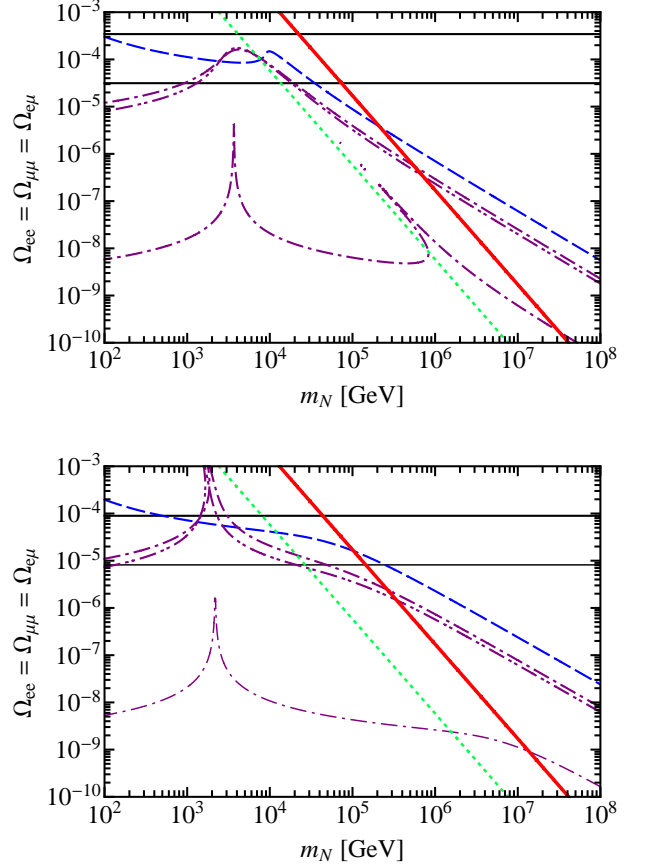


FIG. 2: Exclusion contours of $\Omega_{e\mu}$ versus m_N derived from experimental limits on $B(\mu^- \rightarrow e^- \gamma)$ (solid), $B(\mu^- \rightarrow e^- e^- e^+)$ (dashed) and $\mu \rightarrow e$ conversion in Titanium (dash-dotted) and Gold (dash-double-dotted), assuming $\Omega_{ee} = \Omega_{\mu\mu} = \Omega_{e\mu}$ and $\Omega_{\tau\tau} = 0$. In the lower panel, the quantum effects due to $\tilde{N}_{1,2,3}$ have been ignored. The areas that lie above the contours are excluded; see the text for more details.

on $B(\mu \rightarrow e \gamma)$ provides no useful information for our low-scale SUSY seesaw scenario. However, the upgraded MEG experiment [6] will successfully explore this kinematic region, along with the future PRISM experiment for $R_{\mu e}^{\text{Ti}} \sim 10^{-18}$ [7] which will reach sensitivities to the unprecedented level of $\Omega_{e\mu} \sim 10^{-10}$ and $m_N \sim 10^8$ GeV. In the kinematic regime of large Yukawa couplings, we see that the derived bounds on $\Omega_{e\mu}$ and m_N are much stricter in the SUSY rather than in the non-SUSY case (lower panel). The reason is that in this large m_N domain, $(F_Z^{l'l})^N$ prevails over $(F_Z^{l'l})^{\tilde{N}}$ and adds constructively to the dominant contribution $(F_{\text{box}}^{\mu euu})^N$.

We now turn our attention to τ LFV, analyzing a conservative scenario with $\Omega_{ee} = \Omega_{\tau\tau} = \Omega_{e\tau}$ and $\Omega_{\mu\mu} = 0$ [29]. In Fig. 3 we display exclusion contours of $\Omega_{e\tau}$ versus m_N , using the present experimental upper limits [25] on $B(\tau^- \rightarrow e^- \gamma) < 1.1 \times 10^{-7}$ (solid

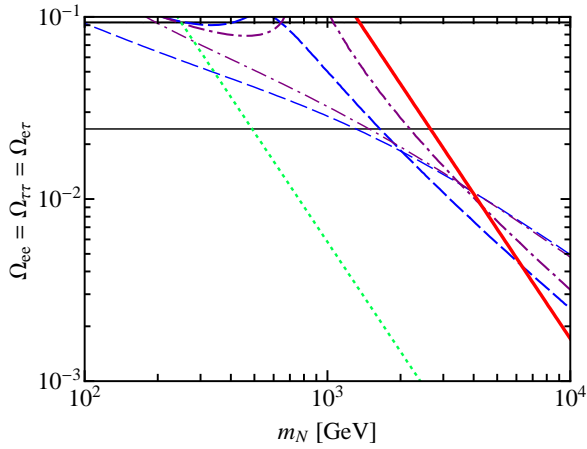


FIG. 3: Exclusion contours of $\Omega_{e\tau}$ versus m_N derived from present experimental upper limits on $B(\tau^- \rightarrow e^- \gamma)$ (solid), $B(\tau^- \rightarrow e^- e^- e^+)$ (dashed) and $B(\tau^- \rightarrow e^- \mu^- \mu^+)$ (dash-dotted), assuming that $\Omega_{ee} = \Omega_{\tau\tau} = \Omega_{e\tau}$ and $\Omega_{\mu\mu} = 0$. More details are given in the text.

lines), $B(\tau^- \rightarrow e^- e^- e^+) < 3.6 \times 10^{-8}$ (dashed lines) and $B(\tau^- \rightarrow e^- \mu^- \mu^+) < 3.7 \times 10^{-8}$ (dash-dotted lines). The thick lines show exclusion contours of SLFV, whereas the thin lines of the same pattern are the corresponding contours in the non-SUSY case. As in Fig. 2, the

diagonal dotted line indicates the regime where large Yukawa coupling effects dominate, whereas the diagonal solid line places the boundary for non-perturbative dynamics. We see that the current bound on $B(\tau \rightarrow e \gamma)$ is not very sensitive to SLFV, in comparison to the other limits on the LFV decay modes of the τ lepton. Moreover, given the constraints [16], a positive signal for $B(\tau^- \rightarrow e^- e^- e^+)$ close to the present upper bounds will signify that SLFV originates from rather large Yukawa couplings and $m_N \gtrsim 3$ TeV.

In summary, we have shown that low-mass right-handed sneutrinos can sizeably contribute to observables of LFV. Thanks to SUSY, they can significantly screen the respective effect of the heavy neutrinos on the photonic μ and τ decays. Hence SLFV can be probed more effectively in the upgraded MEG experiment or in present and future experiments of $\mu \rightarrow e$ conversion in nuclei. The 3-body decay observables, such as $\mu \rightarrow eee$ and $\tau \rightarrow eee$, provide valuable complementary information on SLFV, eliminating a kinematic region that remains unprobed by $\mu \rightarrow e$ conversion experiments. Therefore, plans for potentially upgrading the $\mu \rightarrow eee$ experiment should be followed with the same degree of vigour in the community. In the same vein, we should also explore the implications of SLFV in semileptonic τ decays and in processes involving K and B mesons. We plan to report progress on these issues in the near future.

-
- [1] For reviews, see, H.P. Nilles, Phys. Rept. **110** (1984) 1; H. Haber and G. Kane, Phys. Rept. **117** (1985) 75.
 - [2] P. Minkowski, Phys. Lett. B **67** (1977) 421; M. Gell-Mann, P. Ramond and R. Slansky, in *Supergravity*, eds. D.Z. Freedman and P. van Nieuwenhuizen (North-Holland, Amsterdam, 1979); T. Yanagida, in Proc. of the *Workshop on the Unified Theory and the Baryon Number in the Universe*, Tsukuba, Japan, 1979, eds. O. Sawada and A. Sugamoto; R. N. Mohapatra and G. Senjanović, Phys. Rev. Lett. **44** (1980) 912.
 - [3] F. Borzumati and A. Masiero, Phys. Rev. Lett. **57** (1986) 961.
 - [4] J. Hisano, T. Moroi, K. Tobe and M. Yamaguchi, Phys. Rev. D **53** (1996) 2442.
 - [5] T. P. Cheng and L. F. Li, Phys. Rev. Lett. **45** (1980) 1908.
 - [6] S. Ritt [MEG Collaboration], Nucl. Phys. Proc. Suppl. **162** (2006) 279.
 - [7] Y. Kuno, Nucl. Phys. Proc. Suppl. **149** (2005) 376.
 - [8] D. Wyler and L. Wolfenstein, Nucl. Phys. B **218** (1983) 205.
 - [9] R. N. Mohapatra and J. W. F. Valle, Phys. Rev. D **34** (1986) 1642; S. Nandi and U. Sarkar, Phys. Rev. Lett. **56** (1986) 564.
 - [10] G. C. Branco, W. Grimus and L. Lavoura, Nucl. Phys. B **312** (1989) 492.
 - [11] A. Pilaftsis, Z. Phys. C **55** (1992) 275.
 - [12] A. Pilaftsis, Phys. Rev. Lett. **95** (2005) 081602.
 - [13] J. Bernabéu, A. Santamaria, J. Vidal, A. Mendez and J. W. F. Valle, Phys. Lett. B **187** (1987) 303; J. G. Körner, A. Pilaftsis and K. Schilcher, Phys. Lett. B **300** (1993) 381.
 - [14] A. Ilakovac and A. Pilaftsis, Nucl. Phys. B **437** (1995) 491.
 - [15] F. Deppisch and J. W. F. Valle, Phys. Rev. D **72** (2005) 036001.
 - [16] For the diagonal entries, we conservatively assume that $\Omega_{ee,\mu\mu,\tau\tau} \lesssim 10^{-2}$ [17].
 - [17] S. Bergmann and A. Kagan, Nucl. Phys. B **538** (1999) 368; F. del Aguila, J. de Blas and M. Perez-Victoria, Phys. Rev. D **78** (2008) 013010.
 - [18] A. Ilakovac and A. Pilaftsis, in preparation.
 - [19] We note that unlike the off-shell formfactors, physical amplitudes do not depend on the choice of the gauge.
 - [20] See Appendix B.2 of Haber and Kane in [1].
 - [21] We do not consider here the infra-red singular SUSY limit, without electroweak-symmetry breaking for $\mu \neq 0$.
 - [22] S. Ferrara and E. Remiddi, Phys. Lett. B **53** (1974) 347.
 - [23] H. C. Chiang, E. Oset, T. S. Kosmas, A. Faessler and J. D. Vergados, Nucl. Phys. A **559** (1993) 526.
 - [24] R. Kitano, M. Koike and Y. Okada, Phys. Rev. D **66** (2002) 096002.
 - [25] C. Amsler *et al.*, Phys. Lett. B **667** (2008) 1.
 - [26] To get predictions for $R_{\mu e}$, we use the values for Z_{eff} , $|F(-m_\mu^2)|$ and Γ_{capt} given in [24].
 - [27] SINDRUM II collaboration, C. Dohmen *et al.*, Phys.

Lett. B **317** (1993) 631.

[28] W. Bertl *et al.*, Eur. Phys. J. C **47** (2006) 337.

[29] The limits derived for the complementary scenario with

$\Omega_{\mu\mu} = \Omega_{\tau\tau} = \Omega_{\mu\tau}$ and $\Omega_{ee} = 0$ are quite similar.